This article has been accepted for publication in a future issue of this journal, but has not been fully edited. Content may change prior to final publication. Citation information: DOI 10.1109/TPWRD.2019.2935834, IEEE Transactions on Power Delivery

Experimental validation of a new impedance based protection for networks with distributed generation using co-simulation test platform

Konstantin Pandakov, Charles M Adrah, Hans Kristian Høidalen, Øivind Kure

***Abstract*—Combined real-time hardware-in-the-loop simulations and modeling of communication networks (co-simulation platforms) is a powerful testbed for development and validation of relay protection schemes utilizing communication links especially for applications in Smart Grids. This paper introduces laboratory tests in such environment of a new protection scheme for medium voltage networks with distributed generation. It is based on impedance measurements with compensation of remote infeed currents and high fault resistances. Since the scheme utilizes multi-terminal measurements, a communication network emulator has been developed to model Ethernet network impairments. The test method uses Monte-Carlo approach for evaluation of protection dependability. The results demonstrate enhancement of impedance relay performance compared to the conventional protection. Moreover, fault location capability is preserved with sufficient accuracy. Nevertheless, communication network imperfections, such as jitters and data loss, deteriorate scheme functionality.**

***Index Terms*—co-simulation testbed, distributed generation, HIL, IEC 61850, impedance relaying**

I. Introduction

EXTENSIVE penetration of distributed generation (DG) into distribution networks creates problems for correct operation of the conventional protection mainly based on overcurrent relays. It requires development of new schemes to provide secure network operation.

Impedance (or distance) protection in such case can be an advantageous solution as showed in [1]. [2] demonstrates feasibility of impedance relaying in an actual distribution network. Moreover, it is already a typical practice in several countries [3]. Nevertheless, it is prone to malfunctioning due to underreaching in presence of remote infeed currents from DG and high impedance faults. Hence, the main scope of this study is to present solution for this issue to improve performance of this type of protection in distribution networks.

Impedance protection underreaching was thoroughly investigated in literature with respect to the transmission network where impedance protection is typical. Methods utilizing only local measurements [4]–[9] are of interest since communication technologies and additional equipment is not involved. The methods are aimed at elimination of under- and overreaching issues and offer adaptive settings or error compensation. The main outcome of the methods is possibility to estimate distance to faulty point on the line.

Increased dependability and more accurate results on fault location can be achieved utilizing two-end measurements [4], [10]–[13]. At the same time, synchronized measurements are not necessarily used [12]. A method can also be based on non-fundamental harmonics as in [13].

Special attention is paid to protection of a line between two buses with intertie connection (the third bus) due to difficulties in fault location. Thus, [14] offers adaptive characteristics based on one-end measurements, [15] proposes the scheme utilizing two-end measurements and [16] uses Direct Underreaching Transfer Trip scheme with measurements available from all three terminals. Extensive application of communication links and synchrophasors in a multi-terminal transmission network is considered in [17].

Implementation of these schemes in distribution networks can be problematic because they were mainly developed for high voltage systems with simple configuration (two or three buses), whereas medium voltage (MV) networks have complex topology: several feeders at one substation, side branches and multi-tapped load outfeeds on each feeders, embedded generators. Additionally, performance can also be affected due to: phase of distribution line impedance can reach 45^0 (unlike transmission systems where resistive part is small); fault impedance can be up to several kilo-ohms in case of falling trees [18] (in transmission systems it is typically negligible).

Differential protection schemes can successfully be implemented in distribution networks with DG, for instance [19]; however, information about fault location cannot be provided as with impedance relaying. Furthermore, impact of load currents and current transformer saturation requires careful analysis.

Thus, having advantages of impedance relaying in MV networks, solutions for elimination of its malfunctioning are necessary for development and involvement of communication links facilitates this task. Reference [20] proposes the scheme based on differential impedance (two-point measurements), [21] presents accurate estimation of distance to fault in presence of DG infeed currents, adaptive settings are examined in [22], and [23] studies compensation of DG impact on fault location. One of the shortages here is assumption that the communication networks utilized for realization of the methods are

K. Pandakov is with Department of Electric Power Engineering, Norwegian University of Science and Technology (NTNU), Trondheim, NO-7491 Norway, e-mail: konstantin.pandakov@ntnu.no.

C. M. Adrah is with Department of Information Security and Communication Technology at NTNU, e-mail: charles.adrah@ntnu.no

H. Kr. Høidalen is a professor in NTNU at Department of Electric Power Engineering, e-mail: hans.hoidalen@elkraft.ntnu.no

Ø. Kure is a professor in NTNU at Department of Information Security and Communication Technology, e-mail: okure@ntnu.no

This article has been accepted for publication in a future issue of this journal, but has not been fully edited. Content may change prior to final publication. Citation information: DOI 10.1109/TPWRD.2019.2935834, IEEE Transactions on Power Delivery

ideal, whereas their impact on protection dependability and security is also required to be considered, as for example in [24]. In general, studies in this direction are still lacking.

The current paper, firstly, proposes a new communication-based impedance protection scheme applicable for multi-tapped distribution networks with DG typical for Norway (small-scale hydro power plants). The scheme is capable of compensation of under-reaching errors of impedance measurements caused by remote infeeds and high fault impedances during phase-to-phase faults (with ground path as well if high impedance system grounding is used) utilizing multi-terminal measurements (required, at least, from DG locations). Secondly, this work demonstrates its laboratory verification using real-time (RT) hardware-in-the-loop (HIL) tests. To improve quality and precision of standard HIL tests, a communication emulator has been developed to run together with the RT HIL testbed and to study impact of communication network impairments on overall protection dependability. Furthermore, to evaluate applicability for a real network, a complex network model has been developed for tests to take into account load variations and imbalances. Thus, a new protective scheme can be assessed in close to real-life conditions.

The rest of the paper is organized as follows: Section II briefly outlines the developed compensation strategy (2 particular cases); Section III presents the laboratory co-simulation platform for testing of the protection scheme that includes the real time simulator OPAL-RT®, ABB impedance relay RED 670® and the communication network emulator; the network model with several load points and DG is described in subsection III-A; functionalities and model algorithms of the network emulator are listed in subsection III-B; Section IV introduces the test method including Monte-Carlo simulations for evaluation of method dependability for different conditions; Section V contains the test results with discussions.

II. Overview of Communication-Based Impedance Protection Scheme

A new protection scheme is based on impedance measurements with compensation of errors caused by DG infeed currents and/or high fault impedance. Calculation of impedance errors requires measurements from an embedded generator (typically synchronous) and/or from a remote relay. Depending on network configuration, two cases can be considered.

A. Equivalent line approach (ELA) for compensation of impedance errors

A part of a network between an impedance relay and a remote measuring point (e.g. DG) is passive and has only load outfeeds. In such case, this part before fault is represented as an equivalent line with impedance calculated as $z = (U^{\text{pre}} - U_r^{\text{pre}})/I^{\text{pre}}$, see Fig.1. Here, U and I are phase-to-phase voltage and current respectively, 'pre' denotes prefault conditions and 'r' – remote measurements. Hereafter, phasor quantities are implied. Fault produces an additional node on the equivalent line with voltage U_{err} that is derived from set of equations:

$$\begin{cases} U - U_{\text{err}} = Izk \\ U_r - U_{\text{err}} = I_r z(1-k) \end{cases} \qquad U_{\text{err}} = \frac{UI_r + U_r I - zII_r}{I + I_r}, \quad (1)$$

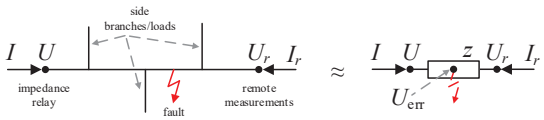

Fig. 1: Example network topology for application of ELA (to the left) and its equivalent (to the right).

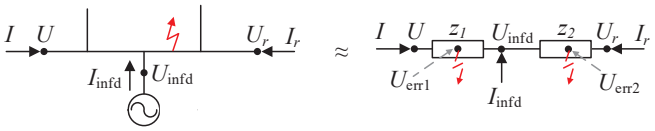

Fig. 2: Example network topology for application of ENA with one infeed source (to the left) and its equivalent (to the right).

where k represents relative distance from the relay to the fault. Current directions are towards the network. The following compensation method of impedance measurements has been proposed:

$$Z_{\text{cps}} = \frac{U - U_{\text{err}}}{I}, \quad (2)$$

where Z_{cps} is the compensated phase-to-phase impedance calculated by the relay and used for tripping decision. Hereafter, it is assumed that Z_{cps} is separately calculated for phases a-b, b-c, and c-a.

B. Equivalent network approach (ENA) for compensation of impedance errors

In this approach, a part of a network between two measuring points is active, that is infeed current from DG is present, see Fig.2. As a result, two passive parts of the network before and after infeed point can be represented for pre-fault conditions as equivalent lines with impedances $z_1 = (U^{\text{pre}} - U_{\text{infd}}^{\text{pre}})/I^{\text{pre}}$ and $z_2 = (U_r^{\text{pre}} - U_{\text{infd}}^{\text{pre}})/I_r^{\text{pre}}$, where U_{infd} and I_{infd} are measured voltage and current at the infeed source. In this case, two probable faulty nodes can exist with voltage error U_{err1} or U_{err2} on each line that can be calculated using the same approach as in (1):

$$U_{\text{err1}} = \frac{U(I_r + I_{\text{infd}}) + U_{\text{infd}} I - z_1 I(I_r + I_{\text{infd}})}{I + I_r + I_{\text{infd}}} \quad (3)$$

$$U_{\text{err2}} = \frac{U_r(I + I_{\text{infd}}) + U_{\text{infd}} I_r - z_2 I_r(I + I_{\text{infd}})}{I + I_r + I_{\text{infd}}}, \quad (4)$$

The smallest among these two determined upon phasor magnitudes is chosen to avoid overcompensation. If U_{err1} is chosen from the minimum condition, then voltage error in equation (2) is equal to $U_{\text{err}} = U_{\text{err1}}$. If U_{err2} is chosen, then an additional voltage drop on equivalent line z_2 caused by DG infeed current must be considered and then voltage error is:

$$U_{\text{err}} = U_{\text{err2}} + kz_2 I_{\text{infd}} = U_{\text{infd}} - \frac{I}{I_r}\left(U_{\text{err2}} - U_r + I_r z_2\right) \quad (5)$$

Equally, measurements at the infeed source can be taken as U_r and I_r in equations (3)-(5), then the remote measurements become U_{infd} and I_{infd}. Having possibility of such swap, two

This article has been accepted for publication in a future issue of this journal, but has not been fully edited. Content may change prior to final publication. Citation information: DOI 10.1109/TPWRD.2019.2935834, IEEE Transactions on Power Delivery

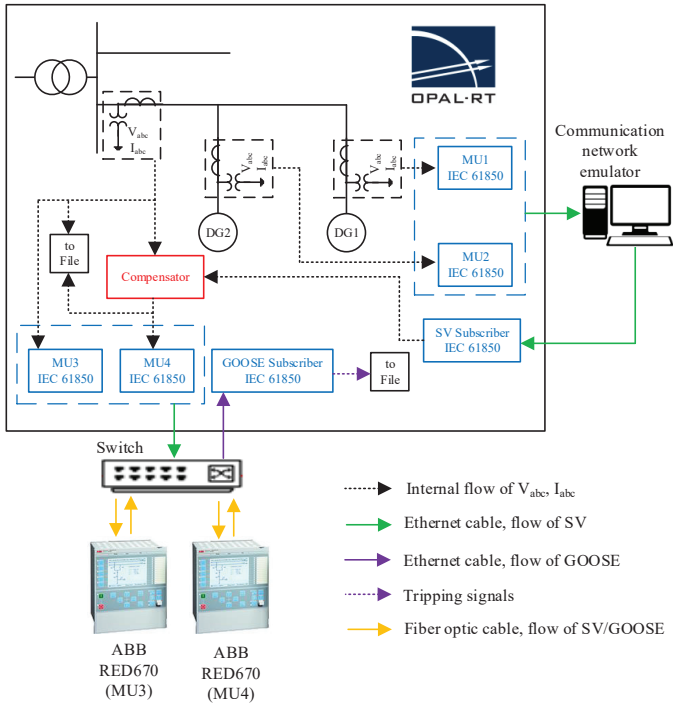

Fig. 3: Laboratory co-simulation testbed: the hardware-in-the-loop testing platform with emulator of communication links.

voltage errors U_{err} for compensation (2) appear. A minimum value (upon magnitude) must be chosen to avoid overcompensation and to increase fault location precision.

General case with several infeed sources and more details can be found in previous work [25].

C. Start conditions for compensation

Voltage error U_{err} is equal to zero during normal conditions in the network, whereas it is nonzero during fault situation recognized upon fulfillment of three conditions together:

1) impedance magnitude measured at relay location falls below a threshold: 80% of what was measured 40 ms ago (two periods). It is expressed as $|U/I| < 0.8|U^{\text{pre}}/I^{\text{pre}}|$.
2) rate of change of this impedance $\frac{\delta|U/I|}{\delta t}$ over the last 5 samples is less than -1 Ohm/ms. Fast collapse indicates a fault.
3) the real part of the impedance is positive that indicates downstream fault (a directional element), $\text{real}(U/I) > 0$.

III. Laboratory Test Setup

Fig.3 shows the full laboratory setup for verification of the proposed method. The previously developed hardware-in-the-loop testing platform [26] is expanded with a communication network emulator [27]. Real time simulations of the network with the DG are executed in OPAL-RT® with 50 μs time step.

Detailed description of the model with 2 embedded generators and fault scenarios are given in the next subsection.

Three-phase voltage and current measurements at the generators and the substation are formed as sample values (SV) in the merging units (MU) using the standard IEC 61850. SV measured at the substation are directly sent to ABB relay RED 670® via MU3 in order to examine impact of the DG on impedance measurements. SV measured at the generators (MU1-2) are sent to the communication network emulator. It models constant time delays, jitters, data loss and background traffic in the SV flows imitating real time communication links (more details are given in subsection III-B). The emulator sends the obtained SV back to the real time simulator (SV Subscriber). The MUs and the subscribers have 4 kHz sampling rate, quality of SVs is set as good.

The compensator accomplishes calculations described in section II, namely: it determines phasors utilizing the obtained SV from the substation and both generators, calculates $U - U_{\text{err}}$ and converts it into an instantaneous signal. This signal together with the measured current at the substation are formed as SV in MU4 and sent to another impedance relay with the same configuration.

In this work, time stamp on SV is not applied assuming unavailability of GPS signal (non-synchronized measurements). Thus, the compensator takes into account known permanent latencies t_d of the remote measurements superimposed by the emulator: $t_d = 3$ ms for DG1 and $t_d = 2$ ms for DG2 have been chosen based on DG remoteness.

Thus, responses (missing or presence of the tripping signals) of the relays with and without compensation are compared: they send GOOSE messages back to the real time simulator (GOOSE Subscriber). The tripping signals and the SV are written to file for further off-line analysis.

The relay settings have Zone 1 not reaching the DG units to allow keeping the feeder alive during DG internal faults and Zone 2 covering the whole feeder and providing backup protection. Zone 1 has positive sequence impedance 13.5+13.5i Ohm with 20 ms time delay for coordination with load fuses; Zone 2 has 20.5+20.5i Ohm. Its time delay must be bigger than breaking operation at the DG units; however, for simplicity and test quickness, 40 ms is set. The zones' boundaries are depicted in Fig.4. The quadrilateral relay characteristics have forward direction and preset fault resistance 10 Ohm because expected maximal arc resistance estimated on Warrington's formula [28] is 7.5 Ohm.

A. Test case network

The test case network is illustrated in Fig.4. The network configuration is specially designed to study impact of load points and infeed current sources (as well as their remoteness from the impedance relay) on both compensation approaches. The network model has been realized in Matlab Simulink®, and all model parameters, described in Table I, are taken from a real Norwegian distribution network (modelled network size is comparable with the real).

Lines 'TL' are modeled as PI-equivalents due to short line lengths and interest in slow transients (up to 1 kHz).

Loads 'Ld' have a random level of active power P and imbalance. Load imbalance at the given load point is modeled as phase-to-phase loads with values equal to 100%, 80% and 120% (between randomly determined phases) from $P/3$. Each load point is independently determined. Thus, overall load profile and imbalance on the feeder alternates. Phase voltage

This article has been accepted for publication in a future issue of this journal, but has not been fully edited. Content may change prior to final publication. Citation information: DOI 10.1109/TPWRD.2019.2935834, IEEE Transactions on Power Delivery

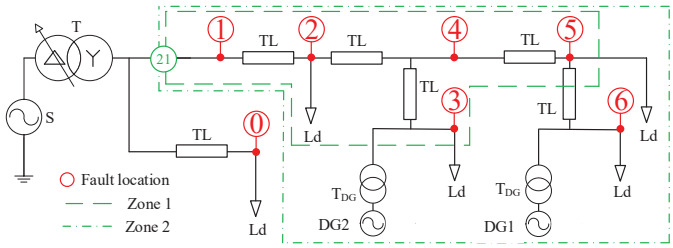

Fig. 4: The test case network.

TABLE I: Network parameters.

	Matlab Simulink model name: parameters
S	Three-Phase Source: 66 kV, 50 Hz, 0.055 H (source inductance)
T, T_{DG}	Three-Phase Transformer (Two Windings): 50 Hz, Rm=500 pu, Lm=500 pu (ideal model) T: 20 MVA, Winding 1 [66 kV 0.0045 pu 0.09739 pu], Winding 2 [22·1.05 kV 0.0045 pu 0.09739 pu] T_{DG}: 3 MVA, Winding 1 [6.6 kV 0.0066 pu 0.06336 pu], Winding 2 [22 kV 0.0066 pu 0.06336 pu]
TL	Three-Phase PI Section Line: 50 Hz, [r1 r0]=[0.36 0.5] Ohms/km, [l1 l0]=[1.146 5.093] mH/km, [c1 c0]=[10.137 4.794] nF/km, length 10 km
Ld	Three-Phase Parallel RLC Load: Delta configuration, 22 kV, 50 Hz, power factor 0.98, Qc=0, total active power is randomly set as 1 MW, 2 MW or 3 MW, 80% imbalance (see description below)
DG1,2	Synchronous Machine: 3 MVA, 6.6 kV, 50 Hz, [Xd Xd' Xd" Xq Xq" Xl]=[2 0.22 0.2 1.4 0.2 0.18] pu, [Tdo' Tdo" Tqo"]=[4 0.025 0.1] s (open circuit), Rs=5e-3 pu, [H(s) F(pu) p]=[1 0 2] Excitation System: IEEE type 1 (default parameters), Hydraulic Turbine and Governor: default parameters

unbalance in the network does not exceed 2% according to EN50160. Randomness is realized using block 'Random Source' with uniform distribution and not repeatable automatic initial seed.

The interconnected generators are operated with zero reactive power production (unit power factor).

Phase-to-phase permanent faults are applied in 7 different locations as shown in Fig.4 with detectable low resistance (an arc with 10 Ohm) and undetectable high resistance (an extraneous object with 50 Ohm causing intentional relay underreach).

B. Communication network emulator

Testing of protection algorithms utilizing inter-substations or even wide area networks requires modeling of communication network impairments to study their impact on overall performance. At the same time, OPAL-RT® has limited capabilities for these purposes. Thus, the communication emulator is proposed to be used together with the RT simulator to mirror behavior and characteristics of communication network properties that tend to have effects in the real-world applications.

The core functionality is to emulate communication network infrastructure between several distant relays exchanging GOOSE/SV packets or messages (fibre-optic point-to-point connections between the substations) so that the communication properties between source relays and destination relays can be varied. These properties are regarded as impairments in the network and include delays, jitters, packet losses, packet corruptions, bandwidth restriction. Additionally, the emulator as a software router can direct packets to actual existing routers and other network elements such as switches, bridges and hubs for integration into real networks. Hence, the emulator is also used to achieve different queuing schemes with different priorities, as well as different router scheduling algorithms.

Network impairments applied in the current work are as follows:

1) Random delay emulator element: It is used to emulate jitters and the input is a specific range for random delays expressed further in the paper using DG permanent latency t_d. Jitters are referred to as variations in latency of data packets. Two jitter levels are used in the tests: 1) the low level when an actual delay is between t_d and $1.5t_d$); 2) the high level when an actual delay is between t_d and $2t_d$. Normal distribution is used.

2) Burst packet drop emulator element: It is used to emulate packet losses. It drops a consecutive number of packets with a given probability. The input is a number of consecutive packets to drop and a probability. Similarly, two data loss levels are used: 1) the low level where 10% on average of packets sending during 1 s are lost; 2) the high level where 20% on average of packets are lost during the same period.

3) Influence of background traffic and network dimension: The generated SV of MU1 and MU2 is sent through the emulator combined with a VLAN enabled switch network (HPE 1920) to the OPAL-RT® simulator. A separate background traffic generated as a User Datagram Protocol (UDP) video source is added to the network traffic mix. The network configurations utilizes the IEEE 802.1Q and IEEE 802.1p priority tagging to investigate how prioritizing the background traffic will affect the performance of the received SV from MU1 and MU2.

IV. Test Method

In order to evaluate dependability and security of the tested protection scheme, a Monte Carlo simulation approach is used that applies several consecutive faults in arbitrary set conditions. The following repeatable sequence with a three-seconds period is utilized for each new fault:

- A random source sets load power P and a separate random source (with different seed) determines phases where load imbalance takes place. Settings are applied to all load points independently with their own random sources.
- After end of the transient period caused by load variation (2 s), a fault is initiated between two randomly determined phases. A different random source determines fault resistance: 10 Ohm or 50 Ohm.
- After another 100 ms the fault is cleared followed by a relaxation period of 900 ms.

Thus, the performed compensation techniques can be applied for different fault parameters and network conditions.

In equations (2) - (5), U and I are always measured at the main substation for device number 21 in Fig.4. U_r, I_r, U_{infd}, I_{infd} can belong to either DG1 or DG2 depending on a case below.

The following scenarios are studied:

This article has been accepted for publication in a future issue of this journal, but has not been fully edited. Content may change prior to final publication. Citation information: DOI 10.1109/TPWRD.2019.2935834, IEEE Transactions on Power Delivery

- Case 1: no communication impairments are introduced. DG permanent latencies are taken into account by the compensator.
  - Case 1a: test of equivalent network approach (ENA, section II-B). U_{infd} and I_{infd} are measured at DG1 (the source of infeed), U_r and I_r are at DG2 (a remote end). 100 consecutive faults are simulated.
  - Case 1b: ENA where U_{infd} and I_{infd} are measured at DG2, and U_r and I_r are at DG1 (100 faults).
  - Case 1c: equivalent line approach (ELA, section II-A). U_r and I_r are measured at DG2, and DG1 is disconnected from the grid (100 faults).
  - Case 1d: ELA where U_r and I_r are measured at DG1, and DG2 is disconnected (100 faults).

  Cases 1a-d are repeated for all 7 fault locations, in total 2800 faults for Case 1 have been simulated. Cases 1c and 1d are used to analyze impact of network configuration on ELA fault location precision. Cases 1a and 1b are used for the same purpose for ENA, as well as to verify validity of the criterion for infeed source selection discussed in subsection II-B.
- Case 2 simulates communication link imperfections – the low and the high level of either jitters or data losses. The compensator still applies the predefined DG permanent latencies.
  - Case 2a: ENA with the low (50 faults) and the high (50 faults) jitter level. Infeed source either DG1 or DG2 is automatically specified using the criterion discussed in subsection II-B.
  - Case 2b: ENA with the low (50 faults) and the high (50 faults) data loss level.
  - Case 2c: ELA with disconnected DG1 for the low (50 faults) and the high (50 faults) jitter level.
  - Case 2d: the same as in 2c, but for the low (50 faults) and the high (50 faults) data loss level.
  - Case 2e: repeats 2c, but with disconnected DG2 instead of DG1.
  - Case 2f: repeats 2d, but with disconnected DG2 instead of DG1.

  For analysis, three extreme fault location have been chosen - 1, 3, and 6. In total 1800 faults for Case 2 have been simulated.
- Case 3 studies impact of background traffic on SV delays and packet losses. Faults are not simulated because impact on protection is seen from Case 2. The practical Ethernet switch used in tests has a priority mapping of class of service queues ('pcp' in the text) and the following have been chosen to test: pcp 1 categorizing traffic types as background, pcp 2–best effort and pcp 3–critical applications. Since SV are the time critical traffic, they were tagged with pcp 3. The background traffic was then varied in the network with pcp 1, 2 and 3. Two video files of 3MB and 10MB were used for the tests. Maximum sending speed for them through 1 Gbps Ethernet is 480 Mbps and 710 Mbps correspondingly.

Finally, percentage of successful tripping among all faults in a specific case can be calculated.

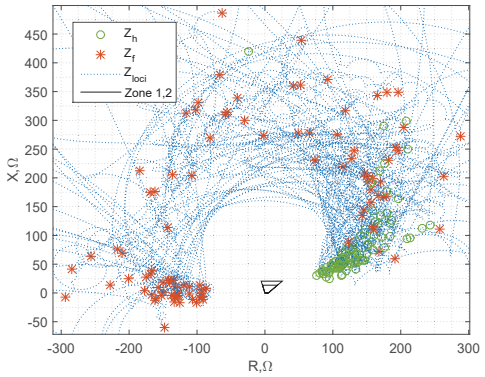

Fig. 5: The impedance loci of faults at location 0 (the adjacent feeder) in test case 1a.

TABLE II: Percentage of successful tripping for Case 1a, 1b.

	FL[1]	Low-ohmic faults				High impedance faults			
		w/o cps[2]		with cps[3]		w/o cps		with cps	
		Z1[4]	Z2[5]	Z1	Z2	Z1	Z2	Z1	Z2
Case 1a	1	100	100	100	100	0	0	100	100
	2	100	100	100	100	0	0	100	100
	3	4	2	82	100	0	0	58	100
	4	100	100	100	100	0	0	100	100
	5	83,7	87,8	100	100	0	0	100	100
	6	0	15,7	74,5	100	0	0	65,3	100
Case 1b	1	100	100	100	100	0	0	100	100
	2	100	100	100	100	0	0	100	100
	3	22,9	10,4	100	100	0	0	96,2	100
	4	100	100	100	100	0	0	100	100
	5	96,4	100	96,4	100	0	0	95,6	100
	6	0	26,5	16,3	100	0	0	11,8	100

[1]fault location, [2]without compensation, [3]with compensation, [4]Zone 1, [5]Zone 2.

V. Results and Discussions

A. Case 1

1) Case 1a and 1b: Firstly, Fig.5 demonstrates impedance loci of faults in the adjacent feeder (location 0) for test case 1a. $Z_{h,f}$ denotes steady-state healthy and faulty impedance correspondingly; upward power flow from the DG can be seen as the negative real part of Z_f. Sympathetic tripping (unnecessary disconnection of the healthy feeder) during the tests has not been registered: all impedance loci are out of zones' reach.

Hereafter, this location is out of interest and excluded from the following analysis because tripping signal is not produced by the investigated relay. Security of the protection is not jeopardized because compensator cannot be initialized due to conditions 1 - 3 in section II-C.

Table II shows calculated percentages of successful tripping in test cases 1a and 1b for fault location 1-6 and two different fault resistances compared to relay performance without the compensation strategy.

The colored cells highlight indices indicating problems: red (relay without compensation) or pink (with) shows decreased dependability (less than 100%), orange - decreased security (higher than 0).

It is seen that low-ohmic fault in location 1,2,4 is reliably detected without compensation in both test cases; however, blinding is observed for high impedance fault because all

This article has been accepted for publication in a future issue of this journal, but has not been fully edited. Content may change prior to final publication. Citation information: DOI 10.1109/TPWRD.2019.2935834, IEEE Transactions on Power Delivery

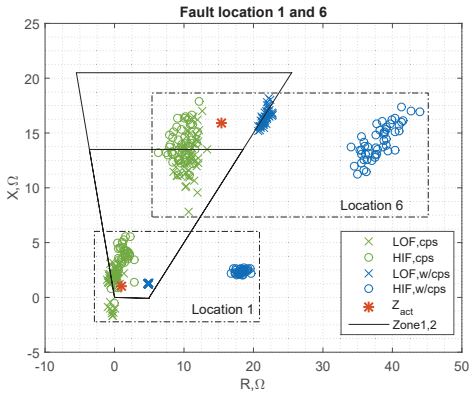

Fig. 6: The measured steady-state fault impedances for low-ohmic (LOF) and high impedance faults (HIF) at location 1 and 6 with compensation (cps) and without (w/cps).

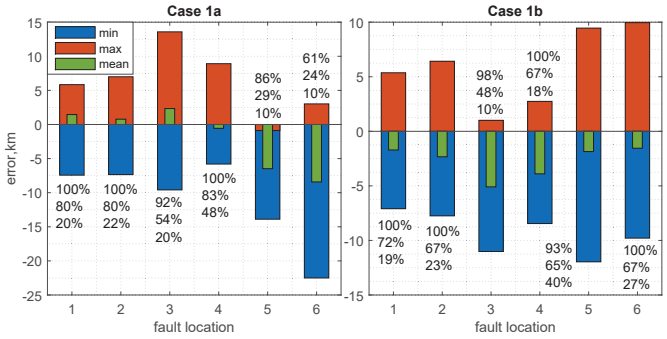

Fig. 7: Fault location errors for Case 1a and 1b (LOF).

locations and cases have 0. At the same time, application of the compensation methods resolves this issue.

We can clearly observe from Table II that relay dependability without compensation is significantly decreased at locations next to the generators (3,5,6). Dependability with compensation is 100% for Zone 2 in all cases, whereas it is not for Zone 1 due to compensation errors that leads to delayed tripping (location 3 for Case 1a and 3,5 for Case 1b).

It is worth noting two main outcomes: 1) Zone 1 must not see faults at location 6 (see Fig.4), whereas in both cases percentage with compensation is not 0 (the orange cells). In other words, the compensated impedance might become smaller than an actual. Since it can lead to a situation when internal faults in DG1 cause unnecessary feeder tripping, the compensator must be blocked to maintain protection selectivity. It can be checked with the same conditions 1 - 3 in subsection II-C applied to measurements at the DG locations: if they are not fulfilled (current is measured towards the monitoring zone), the compensation is not used for the feeder relay; 2) performance of the compensation method in Case 1a is slightly better than in Case 1b for location 5, whereas it is considerably worse for location 3 and 6. As it will be shown further, it is linked with fault location accuracy.

Finally, protection with compensation demonstrates faster operation time: mean value is 40 ms for Zone 1 and 60 ms for Zone 2 irrespectively of fault location and resistance. Without compensation, it can reach 90 ms for problematic locations 3, 5, and 6.

Fig.6 demonstrates the reason for poor relay dependability without compensation and improvements applying ENA (Case 1a is considered) for close-in fault location 1 and far-end location 6. It is seen from the figure that all high impedance faults (HIF) without compensation are out of the zones' reach. Zone 1 can handle all low-ohmic faults (LOF) at close-in location, whereas Zone 2 cannot detect all faults at far-end location due to impact of the DG. 'Z_{act}' denotes an actual fault impedance. The compensated impedances are inside the zones and they have inherent errors with bigger dispersion due to influence of variable network conditions that is the reason of dependability and security issues in Table II. Though for location 1 not all Z_{cps} are in Zone 1, a corresponding locus crosses it and, therefore, the tripping signal appears.

The main advantage of the strategy compared to differential protection is preserving of fault location capability. It is seen from Fig.6 that Z_{cps} for location 1 and 6 are distinguishable, and it is of interest to analyze impact of the compensation on fault location accuracy for all cases.

There are many different approaches for fault location calculation in distribution networks with distributed generation. In this paper, we use a simple one based on the imaginary part of the compensated impedance discussed in [29]. Combination of the compensation strategy with more complex locating algorithms is out of the scope of this paper.

Error in kilometers can be calculated as $\text{imag}(Z_{cps} - Z_{act})/\text{r1}$, where $\text{r1} = 0.36$ Ohm/km (Table I), and Z_{cps} is registered when the tripping signal from Zone 1 or 2 appears, or just a steady-state value if no response is present.

Fig.7 illustrates maximum, minimum and mean errors for 6 fault locations. LOF is considered because it has better precision. For better insight, number of fault incidents (in % from the total) that have a given precision are given alongside: the upper value is precision ± 10 km, the middle is ± 5 km and the lower is ± 2 km.

It can be seen from the plots that the precision for remote locations 5 and 6 is better (compare corresponding indices and mean values) for Case 1b, whereas Case 1a demonstrates better accuracy for location 3. At the same time, average U_{err} for Case 1a is less than for Case 1b during fault at location 3, and it is less for Case 1b for fault at location 5 and 6. Thus, such criterion based on minimum U_{err} (discussed in subsection II-B) can be applied for infeed selection because it provides higher Z_{cps} and, consequently, better fault location accuracy.

To summarize, the presented results in Table II (the pink and orange cells) and in Fig.7 are in good agreement with theoretical expectations: if DG1 is a source of infeed (Case 1a), then locations 5 and 6 are seen as location 4 that gives better dependability and worse security because location 4 is in Zone 1. However, it leads to bigger fault location errors with a negative sign. At the same time, location 3 is detected with some errors leading to the decreased dependability. The opposite is true if an infeed source is DG2 (Case 1b): location 3 is seen as 4 (therefore errors are higher and dependability is better), and 5 and 6 have better location precision (therefore worse dependability and better security).

This article has been accepted for publication in a future issue of this journal, but has not been fully edited. Content may change prior to final publication. Citation information: DOI 10.1109/TPWRD.2019.2935834, IEEE Transactions on Power Delivery

TABLE III: Percentage of successful tripping for Case 1c, 1d.

	FL	Low-ohmic faults				High impedance faults			
		w/o cps		with cps		w/o cps		with cps	
		Z1	Z2	Z1	Z2	Z1	Z2	Z1	Z2
Case 1c	1	100	100	100	100	0	0	100	100
	2	100	100	100	100	0	0	100	100
	3	74,4	67,4	100	100	0	0	100	100
	4	100	100	100	100	0	0	100	100
	5	100	100	100	100	0	0	100	100
	6	0	97,7	100	100	0	0	100	100
Case 1d	1	100	100	100	100	0	0	100	100
	2	100	100	100	100	0	0	100	100
	3	100	100	100	100	0	0	100	100
	4	100	100	100	100	0	0	100	100
	5	100	100	100	100	0	0	95,8	100
	6	0	5,7	45,3	100	0	0	36,2	100

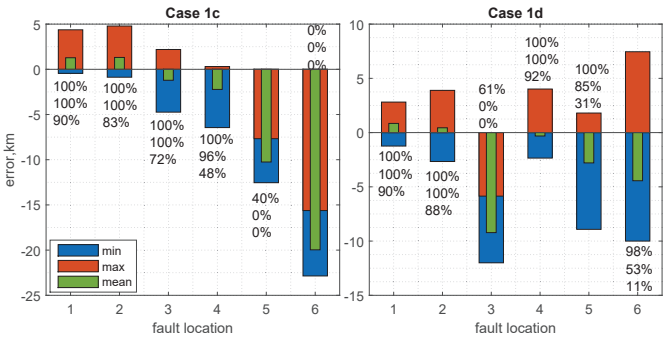

Fig. 8: Fault location errors for Case 1c and 1d (LOF).

2) Case 1c and 1d: Table III shows relay dependability in test cases 1c and 1d. Case 1c shows impact of DG2 (DG1 is disconnected) on relay performance without compensation. As a consequence, dependability reduction is seen for fault location 3,6 and HIF gives 0 as in the previous cases. Case 1d illustrates impact of DG1 seen for location 6. Compensation entirely improves indices for Case 1c, whereas HIF at location 5 has some difficulties for detection by Zone 1 in Case 1d. In both cases, relay security is deteriorated for location 6 (non zero indices for Zone 1). The same point about compensation blocking as in the previous cases is applied here. Finally, protection with compensation is also faster.

Fig.8 shows fault location errors. Case 1c has bigger errors for location 5,6 than Case 1d (zero indices mean large error), but better precision for location 3. This is in agreement with theory because if DG1 is disconnected, then locations 5,6 are seen as 4 (therefore large negative errors in Case 1c) and location 3 is correctly determined; therefore, in Table III, security at location 6 is completely disrupted. If DG2 is disconnected, then the opposite situation arises: location 3 is seen as 4 with large negative error (Case 1d), better security at location 6 and worse dependability for 5 is due to better location accuracy.

To summarize, LOF or HIF inside the zone of protection are reliably detected (at least by Zone 2) with application of the equivalent line or network approach. The main advantage compared to differential protection is preserved fault location capability since errors of impedance measurements can be compensated especially for HIF. For both approaches, the main source of location errors is load currents that are not directly compensated by the given method of equivalences. Accuracy can be improved applying the compensated measurements and the methods discussed in [29].

TABLE IV: Percentage of successful tripping for Case 2a, 2b.

FL	Level	Case 2a (jitters)				Case 2b (data loss)			
		LOF		HIF		LOF		HIF	
		Z1	Z2	Z1	Z2	Z1	Z2	Z1	Z2
1	no[1]	100	100	100	100	100	100	100	100
	low	100	100	100	100	100	100	100	100
	high	81,8	100	85,7	100	95,5	100	100	100
3	no	100	100	96,2	100	100	100	96,2	100
	low	3,3	76,7	5	65	100	100	100	100
	high	0	15	0	10	20,8	83,3	26,9	76,9
6	no	16,3	100	11,7	100	16,3	100	11,8	100
	low	0	53,8	0	62,5	82,6	95,7	11,1	100
	high	0	20,7	0	23,8	18,8	75	14,7	55,9

[1]no impairments.

TABLE V: Percentage of successful tripping for Case 2c, 2d.

FL	Level	Case 2c (jitters)				Case 2d (data loss)			
		LOF		HIF		LOF		HIF	
		Z1	Z2	Z1	Z2	Z1	Z2	Z1	Z2
1	no	100	100	100	100	100	100	100	100
	low	100	100	100	100	100	100	100	100
	high	100	100	71,4	100	100	100	100	100
3	no	100	100	100	100	100	100	100	100
	low	0	88,9	0	82,6	14,3	91,4	13,3	66,7
	high	0	50	0	0	42,9	100	41,4	96,6
6	no	100	100	100	100	100	100	100	100
	low	27, 3	100	0	94,1	78,6	100	77,3	90,9
	high	0	38,5	0	0	78,3	100	66,7	96,23

B. Case 2

This sections demonstrates impact of communication network imperfections, namely jitters and data packet loss, on performance of the compensation methods. Here, fault locations 1,3 and 6 are only considered as extreme points.

1) Case 2a and 2b: Table IV demonstrates performance of the compensation in test cases 2a and 2b compared to similar in Case 1 (without jitters and data loss). The pink colored cells show dependability deterioration compared with cases without communication network distortions, blue - affected security (location 6 only), and the green cells indicate improvements.

Jitter level rise (Case 2a) significantly aggravates relay dependability in locations 3 and 6. Analysis of fault location errors shows that it leads to compensated impedance increase (especially reactive part that deteriorates fault location accuracy) and, consequently, underreaching; therefore, for location 1, influence is not so prominent.

Data loss level rise (Case 2b) has also similar impact – relay dependability falls. Considerable influence is observed for location 3 and 6 for the highest probability.

Improvements are observed for protection security with jitter rise; however, worsening for data loss. At the same time, if the tripping signal appears, operation time is not affected by the communication impairments.

2) Case 2c and 2d: Table V shows results for impact of jitters and data loss in test cases 2c and 2d on the equivalent line approach with disconnected DG1. Comparison with the corresponding results in Case 1 are also present.

As it is possible to observe for location 1, dependability is less than 100% only for the high jitter level and HIF. Impact

This article has been accepted for publication in a future issue of this journal, but has not been fully edited. Content may change prior to final publication. Citation information: DOI 10.1109/TPWRD.2019.2935834, IEEE Transactions on Power Delivery

TABLE VI: Percentage of successful tripping for Case 2e, 2f.

FL	Level	Case 2e (jitters)				Case 2f (data loss)			
		LOF		HIF		LOF		HIF	
		Z1	Z2	Z1	Z2	Z1	Z2	Z1	Z2
1	no	100	100	100	100	100	100	100	100
	low	100	100	100	100	100	100	100	100
	high	95,4	100	21,4	100	100	100	100	100
3	no	100	100	100	100	100	100	100	100
	low	14,8	92,6	0	69,6	69	100	9,5	85,7
	high	0	24,1	0	0	100	100	100	100
6	no	45,3	100	36,2	100	45,3	100	36,2	100
	low	0	38,9	0	3,1	34,5	93,1	23,8	90,5
	high	0	0	0	0	10,7	92,9	4,5	90,9

is less than in Cases 2a,b because only one communication channel is affected. More serious consequences from jitter and data loss level rise are seen for locations 3 and 6. At the same time, clear falling tendency is present with increase of jitter level (Case 2c); however, for data loss (Case 2d), this dependency is not revealed. Finally, location 6 has higher dependability indices due to the applied ELA: it is seen by the fault locating algorithm closer to location 4. In such case, communication network impairments have positive impact on security. Impact of communication link imperfections on location errors is the same as in the previous cases.

3) Case 2e and 2f: Table VI illustrates results for the same ELA as before but DG2 is disconnected. Here impact of the jitters on location 1 is seen even for LOF, and it is higher for HIF than in the previous case. The reason is that calculation errors increase with the distance between two measuring points.

Performance at location 3 is better (indices are higher) than in the previous case because location 3 is now seen as 4; however, impact of network impairments for location 6 is considerable compared to the previous case due to calculation errors of the applied ELA. Positive impact on security in such case is also higher.

To summarize, the main reason of dependability issues in the considered cases is the presence of errors during calculation of the compensated impedance caused by non-synchronized remote measurements or information losses. The analysis of cases with jitter level variation (Case 2a,c,e) can be useful for utilities for evaluation of protective scheme dependability and security in case of sudden loss of synchronizing signal or its unavailability (e.g. underground substations). Data losses have overall adverse effect on the protective schemes increasing relay underreach (Case 2b,d,f); therefore, communication network reliability must be sufficient with minimal packet losses. Finally, comparing results in test Case 2 and Case 1, it is possible to see that even with unreliable communication, protection performance with compensation is superior than without especially for HIF and for LOF in case of low level impairments.

C. Case 3

Fig.9 shows results for test Case 3: end-to-end time delays as mean values over 400000 SV packets with the standard deviation (denoted as 'std') and percentage of lost packets measured between the substations for DG1 and DG2 merging units (MU1 and MU2 respectively) for the two background

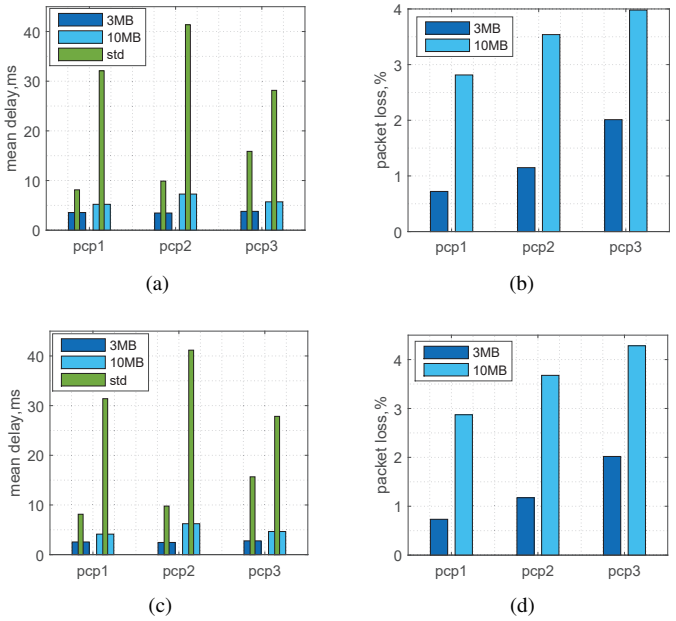

Fig. 9: Impact of 3MB and 10 MB background traffic set with priority (pcp) 1, 2 and 3 on a) end-to-end delays (MU1), b) percentage of lost packets (MU1), c) end-to-end delays (MU2), d) percentage of lost packets (MU2).

sources used in the tests, i.e. 3 MB (maximum 48% traffic occupancy) and 10MB (maximum 71% traffic occupancy) video file sizes, while varying the priority tags of the background traffic as previously explained.

It can be seen that the background traffic with different priority increases end-to-end delays because the mean values are higher than preset (3 ms for MU1 and 2 ms for MU2). Moreover, the 10MB video file as a background traffic source resulted in a generally higher increase in average network delays and standard deviation compared to the 3MB video file. Setting the background traffic with different priority tags has resulted in different packet delay variations; however, a strict regularity is not observed due to randomness nature of packet delays.

Influence of the background traffic on packet losses is seen from Fig.9b and Fig.9d: the 10MB video background traffic generally resulted in more packet losses compared to the 3MB video file. Unlike the previous case, a correlation between pcp and lost packets is prominent. Thus, setting the background traffic as critical messages with pcp = 3, same as the SV traffic for DG1 and DG2, has resulted in the highest percentage of lost packets in the network for both background traffic cases, i.e. MU1 (2.01%, 3.98%) and MU2 (2.01%, 4.28%).

VI. Conclusion

The current paper, firstly, presents a new communication-assisted impedance-based protective scheme for distribution grids with DG and, secondly, its comprehensive laboratory tests using the developed co-simulation platform that includes a real time hardware-in-the-loop testbed and a network emulator. The latter creates controlled communication network

parameters for protection testing in close to real life environment.

The protection scheme aims at elimination of underreaching errors during impedance measurements associated with DG and high impedance faults. It demonstrates promising results with ideal communication links improving dependability compared to the conventional distance relaying. The test results also reveal negative impact of communication network impairments, such as uncompensated jitters or data losses, leading to underreaching errors especially for far end fault locations. Hence, the main limitation of the developed protection scheme is communication links quality and reliability.

Though the tests show that unbalanced and dispersed load currents have impact on fault location accuracy, faulty points can be differentiated due to utilization of prefault measurements in the method and large synchronous generator fault currents exceeding load currents. The latter means that in networks with inverter-integrated DG fault location errors might be bigger, but since it leads to relay overreaching, protection scheme dependability should stay high. Further investigations in this direction are required.

ELA can only be applied for a passive network between two-point measurements (Fig.1). If a network becomes active, ENA is used (Fig.2) since multiple-point measurements are required. As it is seen from the analysis, the main disadvantage of both approaches is recognition of faults in lateral branches in false locations (on the feeder). If more precise fault discrimination is needed, additional measurements in these branches can be provided. Therefore, a large network with complex topology and scattered DG sources is divided into several zones of protection where ELA or ENA can be applied. In order to select a correct (i.e. that gives the best fault location precision) remote relay for calculation of Z_{cps} in both approaches, the criterion of minimum U_{err} or maximum Z_{cps} must be applied. Finally, the results reveal that ELA demonstrates better fault location accuracy than ENA and less susceptibility to communication network imperfections, therefore it must be prioritized.

REFERENCES

[1] A. Sinclair, D. Finney, D. Martin, P. Sharma. (2014). Distance Protection in Distribution Systems: How It Assists With Integrating Distributed Resources. *IEEE Transactions on Industry Applications. 50(3)*, pp. 2186 – 2196.

[2] K. Pandakov, H. Kr. Høidalen, J.I. Marvik, "Implementation of distance relaying in distribution network with distributed generation", *13th International Conference on Development in Power System Protection (DPSP)*, 2016, pp. 1 – 7.

[3] Joint Working Group B5/C6.26/CIRED. (2015) *Protection of Distribution Systems with Distributed Energy Resources*.

[4] M. M. Saha, J. Izykowski, E. Rosolowski, M. Bozek, "Adaptive Line Distance Protection with Compensation for Remote End Infeed", *IET 9th International Conference on Developments in Power System Protection (DPSP)*, 2008, pp. 1 – 6.

[5] V.H. Makwana, B. Bhalja. (2012). New digital distance relaying scheme for phase faults on doubly fed transmission lines. *IET Generation, Transmission & Distribution. 6(3)*, pp. 265 – 273.

[6] V. H. Makwana, B. R. Bhalja. (2012). A New Digital Distance Relaying Scheme for Compensation of High-Resistance Faults on Transmission Line. *IEEE Transactions on Power Delivery. 27(4)*, pp. 2133 – 2140.

[7] Y. Zhong, X. Kang, Z. Jiao, Z. Wang, J. Suonan. (2014). A Novel Distance Protection Algorithm for the Phase-Ground Fault. *IEEE Transactions on Power Delivery. 29(4)*, pp. 1718 – 1725.

[8] Z. Y. Xu, G. Xu, L. Ran, S. Yu, Q. X. Yang. (2010). A New Fault-Impedance Algorithm for Distance Relaying on a Transmission Line. *IEEE Transactions on Power Delivery. 25(3)*, pp. 1384 – 1392.

[9] Q. K. Liu, S. F. Huang, H. Z. Liu, W. S. Liu. (2008). Adaptive Impedance Relay With Composite Polarizing Voltage Against Fault Resistance. *IEEE Transactions on Power Delivery. 23(2)*, pp. 586–592.

[10] M.M. Eissa. (2006). Ground distance relay Compensation based on fault resistance calculation. *IEEE Transactions on Power Delivery. 21(4)*, pp. 1830 – 1835.

[11] T. G. Bolandi, H. Seyedi, S. M. Hashemi, P. S. Nezhad. (2015). Impedance-Differential Protection: A New Approach to Transmission-Line Pilot Protection. *IEEE Transactions on Power Delivery. 30(6)*, pp. 2510 – 2518.

[12] Z.Li, X. Lin, H. Weng, Z. Bo. (2012). Efforts on Improving the Performance of Superimposed-Based Distance Protection. *IEEE Transactions on Power Delivery. 27(1)*, pp. 186 – 194.

[13] C. J. Lee, J. B. Park, J. R. Shin, Z. M. Radojevie. (2006). A new two-terminal numerical algorithm for fault location, distance protection, and arcing fault recognition. *IEEE Transactions on Power Systems. 21(3)*, pp. 1460 – 1462.

[14] J. Ma, X. Xiang, P. Li, Z. Deng, J. S. Thorp. (2017). Adaptive distance protection scheme with quadrilateral characteristic for extremely high-voltage/ultra-high-voltage transmission line. *IET Generation, Transmission & Distribution. 11(7)*, pp. 1624 – 1633.

[15] Y. Lin, C. Liu, C. Yu. (2002). A new fault locator for three-terminal transmission lines using two-terminal synchronized voltage and current phasors. *IEEE Transactions on Power Delivery. 17(2)*, pp. 452 – 459.

[16] S. Sarangi, A. K. Pradhan. (2015). Adaptive Direct Underreaching Transfer Trip Protection Scheme for the Three-Terminal Line. *IEEE Transactions on Power Delivery. 30(6)*, pp. 2383 – 2391.

[17] N. A. Al-Emadi, A. Ghorbani, H. Mehrjerdi. (2016). Synchrophasor-based backup distance protection of multi-terminal transmission lines. *IET Generation, Transmission & Distribution. 10(13)*, pp. 3304 – 3313.

[18] N. I. Elkalashy, M. Lehtonen, H. A. Darwish, M. A. Izzularab, A. I. Taalab. (2007). Modeling and experimental verification of high impedance arcing fault in medium voltage networks. *IEEE Transactions on Dielectrics and Electrical Insulation. 14(2)*, pp. 1 – 9.

[19] H. Gao, J. Li, B. Xu. (2017). Principle and Implementation of Current Differential Protection in Distribution Networks With High Penetration of DGs. *IEEE Transactions on Power Delivery. 32(1)*, pp. 565 – 574.

[20] W. Huang, T. Nengling, X. Zheng, C. Fan, X. Yang, B. J. Kirby. (2014). An Impedance Protection Scheme for Feeders of Active Distribution Networks. *IEEE Transactions on Power Delivery. 29(4)*, pp. 1591-1602.

[21] S. Biswas, V. Centeno, "A communication based infeed correction method for distance protection in distribution systems", *North American Power Symposium (NAPS)*, 2017, pp. 1 – 5.

[22] J. Ma, J. Li, Z. Wang, "An adaptive distance protection scheme for distribution system with distributed generation", *5th International Conference on Critical Infrastructure (CRIS)*, 2010, pp. 1 – 4.

[23] J. I. Marvik, H. K. Høidalen, A. Petterteig, "Localization of short-circuits on a medium voltage feeder with distributed generation", *20th International Conference and Exhibition on Electricity Distribution (CIRED 2009) - Part 1*, 2009, pp. 1 – 4.

[24] A. C. Adewole, R. Tzoneva. (2017). Co-simulation platform for integrated real-time power system emulation and wide area communication. *IET Generation, Transmission & Distribution. 11(12)*, pp. 3019-3029.

[25] K. Pandakov, H. Kr. Høidalen. "Distance Protection with Fault Impedance Compensation for Distribution Network with DG", *IEEE PES Innovative Smart Grid Technologies Conference Europe (ISGT-Europe)*, 2017, pp. 1-6.

[26] Z. Liu, H. K. Høidalen. "An adaptive inverse time overcurrent relay model implementation for real time simulation and hardware-in-the-loop testing", *13th International Conference on Development in Power System Protection 2016 (DPSP)*, 2016, pp. 1-6.

[27] C. M. Adrah, Ø. Kure, Z. Liu, H. Kr. Høidalen. "Communication network modeling for real-time HIL power system protection test bench", *IEEE PES PowerAfrica*, 2017, pp. 1-6.

[28] V. D. Andrade, E. Sorrentino. "Typical expected values of the fault resistance in power systems", *Transmission and Distribution Conference and Exposition: Latin America (T&D-LA), 2010 IEEE/PES*, 2010, pp. 1-8.

[29] B. D. S. Jose, P. A. H. Cavalcante, F. C. L. Trindade, M. C. de Almeida. "Analysis of distance based fault location methods for Smart Grids with distributed generation", *IEEE PES ISGT Europe*, 2013, pp. 1-5.